Enhanced diffusion due to motile bacteria

Min Jun Kim and Kenneth S. Breuer[a)]
Division of Engineering, Brown University, Providence, Rhode Island 02912

(Received 6 May 2004; accepted 9 July 2004; published online 6 August 2004)

The effect of bacterial motion on the diffusion of a molecule of high molecular weight is studied by observing the mixing of two streams of fluid in a microfluidic flow cell. We show that the presence of motile *E. coli* bacteria in one of the streams results in a marked increase in the effective diffusion coefficient of Dextran, which rises linearly with the concentration of bacteria from a baseline value of 0.2×10^{-7} to 0.8×10^{-7} (cm^2/s) at a concentration of 2.1×10^9/ml (approximately 0.5% by volume). Furthermore, we observe that the diffusion process is also observed to undergo a change from standard Fickian diffusion to a superdiffusive behavior in which the diffusion exponent rises from 0.5 to 0.55 as the concentration of bacteria rises from 0 to 2.1×10^9/ml. © *2004 American Institute of Physics*. [DOI: 10.1063/1.1787527]

Flagellated bacteria, such as *E. coli* or *Serratia marsescens*, propel themselves by means of several helical flagella, each approximately 6–10 microns long, that are rotated at speeds of approximately 100 Hz by molecular motors embedded in the cell membrane.[1] When the motors all rotate counterclockwise, the flagella coalesce together to form a bundle which propels the organism through the medium at speeds of up to 30 μm/s. When one or more of the rotary motors change direction, the flagellar bundle disperses and the bacteria tumbles, changing direction. Thus the organism executes a random walk.[2] The cell motion induces motion in the surrounding fluid[3] and one would expect that this might have an effect on the transport and diffusion of a passive scalar in the fluid. Wu and Libchaber[4] studied the effect of *E. coli* on micron-scale beads in a freely suspended soap film. They showed that the diffusion of beads is proportional to the concentration of *E. coli*. Through their experiments, large positional fluctuations were observed for beads as large as 10 μm in diameter, and the measured mean-square displacements of the beads grew faster than $\sqrt{t}$ for short times suggesting a superdiffusive behavior. Grégoire *et al.*[5] introduced a simple model for the motion of passive beads in a noisy bath of active "boids" interacting only locally. Their results not only indicate that true superdiffusive motion of both bacteria and bead tracer is present in the bacterial bath but also suggest that superdiffusive behavior should indeed be generically observed due to the onset of collective motion. The present experiment is aimed at exploring this phenomenon in some more detail. However, rather than looking at the diffusion of relatively large particles, we are concerned about the diffusion of macromolecules (in this case Dextran) uniformly distributed in the bulk fluid.

In the current experiment, a PDMS (poly-dimethylsiloxane) microchannel is fabricated using standard soft-lithography techniques[6,7] (Fig. 1). The channel is in the form of a "Y," with two arms each feeding a stream of fluid into a main channel which measures 28 mm long, 40 microns high and 200 microns wide. One arm carries a biological buffer solution, plus a low concentration (0.02% by volume) of Dextran (molecular weight: 77 000) labelled with FITC (fluorescein isothiocyanate). The second side contains the same buffer and Dextran, except that the Dextran is not fluorescently labelled. As the two streams flow down the main channel, the clear boundary that exists between the two streams spreads gradually due to molecular diffusion between the fluid in the two streams. The local concentration of labelled Dextran is proportional to the flourescence intensity across the channel, $I(y)$, measured optically using an inverted microscope stage at 20× magnification using a high-resolution (1300×1030 pixels) cooled charge coupled device (CCD) camera.

Standard diffusion theory,[8] in which we ignore the variations that exist through the depth of the channel and assume that the channel width is large compared to the width of the diffusion zone, predicts that intensity profile across the channel is given by the complementary error function

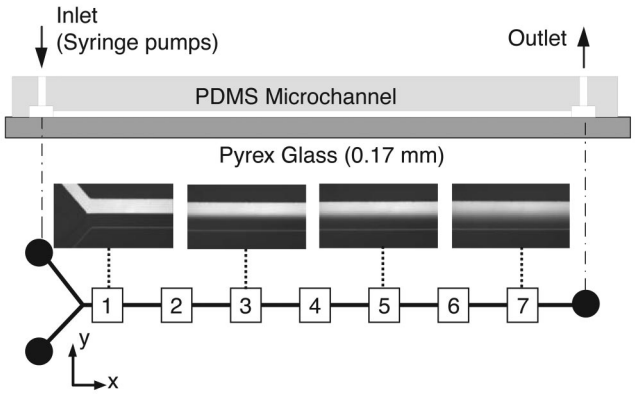

FIG. 1. Schematic of the test geometry, illustrating the microchannel and sample diffusion profiles as they develop along the length of the channel. The channel measures 40 microns deep, 200 microns wide and 28 mm long. In the main channel, we capture images at sections 1 through 7, located at $x=0.5,4,8,12,16,20,24$ min (measured from the Y-junction).

[a)]Author to whom correspondence should be addressed. Telephone: (401) 863-2870; fax: (401) 863-9028. Electronic mail: kbreuer@brown.edu

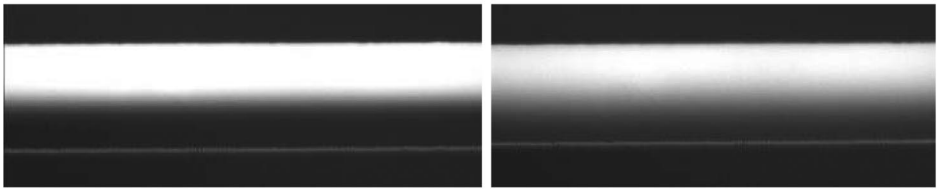

(a) (b)

FIG. 2. Optical micrographs of diffusion profiles for the baseline condition (a) and a condition in which wild-type bacteria were introduced to the upper (fluorescent) stream at a concentration of 1.05×10^9/ml (b). In both cases the flow rate is 0.5 μl/min and the images were captured 24 mm (Section 7) from the Y-junction. The enhancement of mixing is apparent.

$$I(y) = \mathrm{erfc}(\eta) \tag{1}$$

where η is a similarity variable:

$$\eta = \frac{y}{\sqrt{Dx/U}}. \tag{2}$$

D is the molecular diffusion coefficient, U is the average velocity and x is the distance from the mixing origin. The gradient of the intensity profile should behave like

$$\frac{\partial I}{\partial y} = \frac{1}{2\sqrt{\pi Dx/U}} e^{-(y/2\sqrt{Dx/U})^2}, \tag{3}$$

from which one observes that the maximum in the intensity gradient should decay proportional to $(x/U)^{-1/2}$, and that the width of the diffusion zone, measured by the standard deviation of the intensity gradient, should grow proportional to $\sqrt{x/U}$.

Live and highly motile *E. coli* bacteria were introduced at low concentrations into the fluorescent stream and the changes in the diffusion characteristics of the FITC-Dextran were recorded. A sample pair of images from the baseline (no bacteria) and a case with bacteria is shown in Fig. 2. The enhanced diffusion due to the presence of bacteria is apparent. Images such as these were captured using two strains of bacteria: wild-type *E. coli* (strain: HCB 33) and tumbly *E. coli* (strain: RP 1616). The tumbly mutant has active flagella similar in size and performance to the wild-type strain. However, the motors in the tumbly mutant are biased to favor clockwise rotation than the wild type, and for this reason the flagella do not form a coherent bundle and consequently the cells are trapped in a permanent tumble mode and are rarely observed to run. After testing with wild-type *E. coli*, 0.001% of FCCP (carbonylcyanide-p-trifluoromethoxyphenyl hydrazone) was added to the buffer, immobilizing the bacteria. The experiments were then repeated using the de-energized bacteria. A range of dilute bacterial concentrations ($0-2.1\times10^9$/ml) and flow rates (0.5, 0.75, 1.00, 1.25 μl/min) were tested. Measurements were taken at seven x-stations along the mixing channel ($x=0,4,8,12,16,20$ and 24 mm, distances measured from the Y-junction). Intensity profiles, $I(y)$, were generated from the images by averaging over 300 pixels (107 microns) in the streamwise direction and over 10 separate images. The profiles were acquired at different combinations of axial location, flow rate and bacterial concentration.

As an example, Fig. 3(a) shows the gradient of the intensity profile, dI/dy, at several x-locations for a fixed bacterial concentration and flow rate of 1.25 μl/min. The position, x, and average speed, U, can be combined to form a combined variable, $\tau=x/U$, which measures the average time taken by a fluid element to advect at speed U to point x. The maximum of the intensity gradient is observed to be solely a

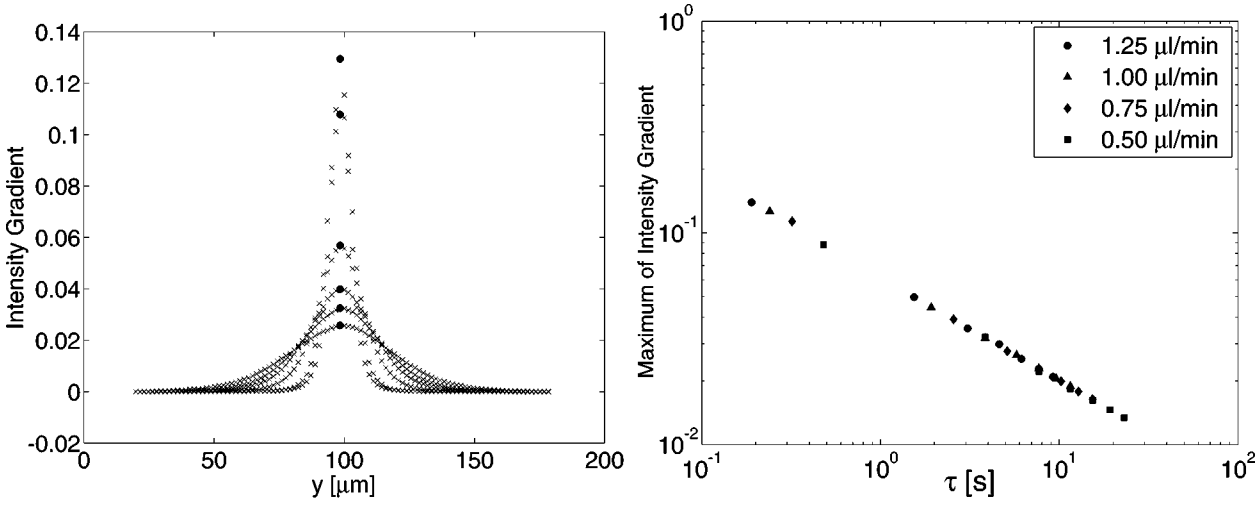

(a) (b)

FIG. 3. (a) Diffusion profiles at different distances from the Y-junction, generated from images for $Q=1.25$ μl/min. (b) The variation of the maximum of the diffusion distribution, from all seven x-locations and four different flow rates, plotted using the combined variable: $\tau=x/U$.

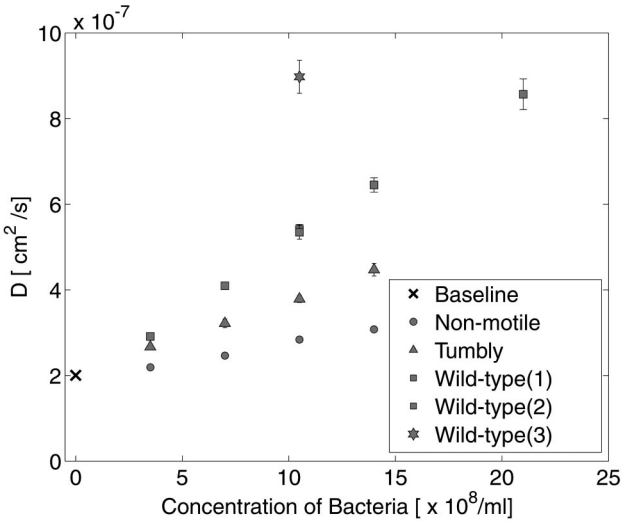

FIG. 4. Variation of the apparent diffusion coefficient, D as a function of the concentration of bacteria, assuming standard diffusion. The effects of adding wild-type *E. coli*, tumbly *E. coli*, and inactive *E. coli* are shown. The baseline case has no *E. coli* present. Three configurations are shown: (1) bacteria are added only to the FITC+Dextran stream, while the nonfluorescent stream is not changed; (2) the fluorescent stream is left untouched while *E. coli* are added to the nonfluorescent stream. The results are identical with the previous configuration, confirming that the presence of the FITC does not affect the results. Lastly, (3) *E. coli* are added to both streams. In this case, the diffusion coefficient is approximately double the case in which bacteria at the same concentration are present in only one stream. The error bars represent the uncertainty in the determination of D.

function of τ, for the full range of x and U tested [Fig. 3(b)], confirming that the diffusion enhancement is independent of the average shear rate established in the system by the flowing streams (which is constant with x, but varies with U), and that the one-dimensional assumption in our analysis (in which we ignore both the shear through the depth of the channel and the weak shear across the width of the channel) is valid.

If we assume that the system follows Fickian diffusion dynamics as discussed above, we can extract the apparent diffusion coefficient, D [Eq. (3)], by least-squares regression analysis. Doing this for all the cases tested yields Fig. 4, which shows D as a function of the bacteria concentration for three different cases: wild-type, tumbly, and de-energized *E. coli*. The effective diffusion coefficient is observed to increase linearly with bacterial concentration and is enhanced by a factor of 4 at the highest bacterial concentration tested (which is still a relatively low volume concentration of bacteria, corresponding to a volume concentration of less than 0.5%). Placing the bacteria in the nonfluorescent stream (instead of the fluorescent stream) has the identical effect, indicating that the FITC tag does not affect the mixing process or the bacterial effectiveness. Finally, seeding both streams with bacteria approximately doubles the effective value of D. All three configurations suggest that the mixing enhancement is due to the local concentration of bacteria in the mixing interface, and not affected by the particular manner in which they are brought there.

The de-energized *E. coli* are also observed to promote an enhanced diffusion of the Dextran which, although much weaker than the enhancement observed with active cells, is nevertheless present. As mentioned above, the results are independent of the average shear rate in system, which would suggest that solute transport due to shear-induced diffusion (either of the Dextran, or of the bacterial cells) is negligible.[9–11] The source of the enhanced transport, which increases linearly with bacterial concentration, might be due to Brownian motion of the inactive cells and their flagella. Enhanced transport due to particles suspended in a flow

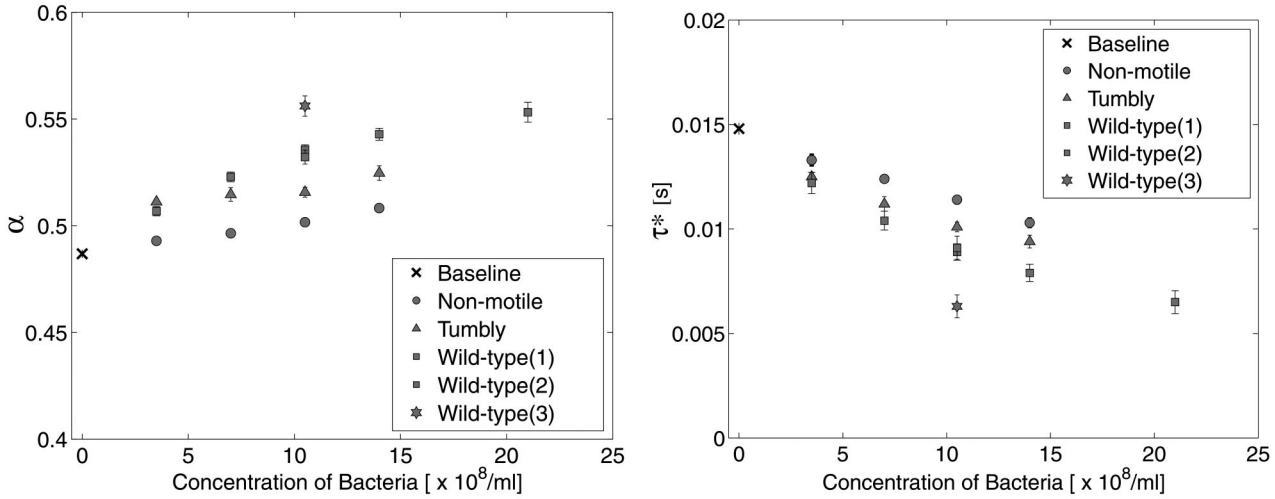

(a) (b)

FIG. 5. Variation of (a) the diffusion rate, α, and (b) the associated time scale, τ_*, as a function of the bacteria concentration. The effects of wild-type *E. coli*, tumbly *E. coli*, and de-energized *E. coli* are shown. The three wild-type configurations are as described in Fig. 4. The error bars represent the uncertainty in the determination of α and τ_*.

without shear has been observed,[12] although we are not aware of extensive investigation of this pheomenon and this needs to be investigated further. The difference between the enhancement due to wild-type and tumbly *E. coli* argues for one of two possible mechanisms responsible for the mixing enhancement: First, the clockwise flagellar motion (more common in the tumbly strain) may be less efficient than the counterclockwise flagellar motion (more common in the wild-type strain). Second, it may be that the motion of the cell body during the coordinated run (only exhibited by wild-type strain) generates a more efficient mixing field than the uncoordinated tumble phase (dominant in the tumbly strain).

A more careful examination of the decay in the intensity gradient [Fig. 3(b)] shows that the slope of the diffusion profile evolution (plotted on log–log axes) deviates from the theoretical value of -0.5 in a small, but consistent, manner and that this slope varies with bacterial concentration. This suggests that a nonconventional diffusion process may be present. Dimensional analysis suggests that the thickness of the diffusion layer, δ, normalized by the thickness at some reference location, can be modelled as

$$\frac{\delta}{\delta_o} \propto \left[\frac{\tau}{\tau_*}\right]^{\alpha}, \tag{4}$$

where α is the diffusion exponent and τ_* is a time scale. For Fickian diffusion, α is equal to 0.5, and τ_* is determined solely by the molecular diffusion coefficient. In the case of nonconventional diffusion, τ_* will also be influenced by non-molecular scales such as the characteristic time between bacteria–bacteria interactions (measured approximately as the mean bacterial separation divided by their average swimming speed). Adopting this model for the diffusion process, we have fit the measured data to this model, finding optimal values for both α and τ_*. The results are shown in Fig. 5, which shows the values of α and τ_*, both as a function of bacteria concentration, c. We find that there is a clear trend of increasing superdiffusion ($\alpha > 0.5$) as the concentration of bacteria increases. An indication of the global error in the experiment is given by the fact that the baseline case ($c = 0$) should be characterized by $\alpha = 0.5$, but instead is found to have $\alpha = 0.49$—a discrepancy of only 2%. In contrast, α is observed to increase smoothly and linearly as c increases, rising to a value of $\alpha = 0.55$ for $C = 2.1 \times 10^9$/ml. Extrapolating this trend predicts $\alpha = 0.74$ at a concentration of 10^{10}/ml—in excellent agreement with the lower estimate for α observed by Wu and Libchaber.[4] The corresponding value of τ_* is also observed to fall, suggesting that as the bacteria become more densely packed, their interaction time falls. However, direct measurements of the actual bacterial motion are needed before one can infer anything about the onset of larger scale cooperative motions that might be responsible for the superdiffusive behavior.

We acknowledge the invaluable contributions of Linda Turner, Nick Darnton, and Howard Berg for access to their bacteria strains, their expertise, advice and experience in culturing and handling and understanding *E. coli*, and to Tom Powers, MunJu Kim, and Jacy Bird for their assistance in performing and interpreting the experiments. This work is supported by the DARPA BioMolecular Motors Program.

[1] H. C. Berg, "Motile behavior of bacteria," Phys. Today **53** (1), 24 (2000).
[2] H. C. Berg and D. A. Brown, "Chemotaxis in *Escherichia coli* analysed by three-dimensional tracking," Nature (London) **239**, 500 (1972).
[3] M.-J. Kim, J. Bird, A.-M. van Parys, K. Breuer, and T. Powers, "A macroscopic scale model of bacterial flagellar bundling," Proc. Natl. Acad. Sci. U.S.A. **100**, 15481 (2003).
[4] X.-L. Wu and A. Libchaber, "Particle diffusion in a quasi-two-dimensional bacterial bath," Phys. Rev. Lett. **84**, 3017 (2000).
[5] G. Grégoire, H. Chaté, and Y. Tu, "Active and passive particles: Modeling beads in a bacterial bath," Phys. Rev. E **64**, 011902 (2001).
[6] G. Whitesides and A. Stroock, "Flexible method for microfluidics," Phys. Today **54** (6), 42 (2001).
[7] D. Duffy, C. McDonald, O. Schueller, and G. Whitesides, "Rapid prototyping of microfluic systems in poly(dimethylsiloxane)," Anal. Chem. **70**, 4974 (1998).
[8] E. Cussler, *Diffusion: Mass Transfer in Fluid Systems* (Cambridge University Press, Cambridge, UK, 1997).
[9] N.-H. L. Wang and K. Keller, "Augmented transport of extracellular solutes in concentrated erythrocyte suspensions in Couette flow," J. Colloid Interface Sci. **103**, 201 (1985).
[10] A. L. Zydney and C. K. Colton, "Augmented solute transport in the shear flow of a concentrated suspension," PCH, PhysicoChem. Hydrodyn. **10**, 77 (1988).
[11] V. Breedveld, D. Vanden Ende, A. Tripathi, and A. Acrivos, "The measurement of shear-induced particle and fluid tracer diffusivities in concentrated suspensions by a novel method," J. Fluid Mech. **375**, 297 (1998).
[12] A. Tripathi and A. Acrivos, "Viscous resuspension in a bidensity suspension," Int. J. Multiphase Flow **25**, 1 (1999).